550.834

SEISMIC MEASUREMENTS OF LARGE UNDERWATER SHOTS

by

REIDAR KANESTRØM and OVE ØVREBØ[1)]

Seismological Observatory
University of Bergen
Bergen, Norway

Abstract

In connection with the seismic refraction experiment carried out in Scandinavia in 1969, nine charges ranging from 1000 to 4000 kg TNT were detonated on the sea floor at various water depths (55 to 140 m). These explosions were recorded at NORSAR, and the amplitude spectra were calculated for the first second of 215 seismograms. The frequency at the maximum value of the spectrum for each shot was close to the theoretical fundamental resonance frequency $f_0 = v/4h$, where v is the velocity of sound in sea water and h is the water depth.

The bubble-pulse period was determined from the evenly spaced minima and maxima in the spectrum resulting from the interference between arrivals from the initial shot pulse and arrivals from the bubble pulse. For this purpose the first six seconds of the seismograms were analysed. The bubble-pulse period determined in this way agrees with that predicted by the Willis' bubble formula.

1. *Introduction*

During the summer of 1969 a large seismic refraction program was carried out in Scandinavia as a joint project between scientists from Denmark, Finland, Norway, Sweden and West-Germany. Nine charges between 1000 and 4000 kg TNT were detonated on the sea floor at depths varying from 55 to 140 m. The seismic waves generated by these shots were recorded by the Scandinavian seismograph network, NORSAR, Hagfors array, and at a large number of field stations spaced along 6 profile lines. Interpretations of the seismic data collected during the experiment

[1)] Present address: Norwegian Petroleum Directorate, N-4000 Stavanger, Norway.

have been published in a number of accounts (BÅTH [1]; BROWN *et al.* [2]; KANESTRØM [5] and VOGEL [13].

Underwater explosions are frequently used in seismic refraction measurements. In order to complete an interpretation of the seismic signals recorded a study of the dynamical properties of the generated waves is necessary. Consequently, the effect of variations in water depth and the size of the charge on the recorded signal must be known. Furthermore, it is important that the bubble-pulse period can be determined so that signals from secondary pressure pulses can be taken into account when interpreting seismic records.

The present paper will be mainly concerned with a presentation of some conclusions reached during the analysis of the seismic signals recorded at NORSAR from the 1969 underwater explosions.

2. *Data*

The location of shot points used in the 1969 seismic experiment is shown in Figure 1, and the source data are given in Table 1. The data used in this study were recorded at the Lillehammer array (LHN) and the following subarrays in NORSAR: 01A, 03B, 07B and 01C. In 1969, NORSAR was under construction and recording equipment had not been installed at the other subarrays. The location of LHN and the subarrays used is shown in Figure 2; Figure 3 shows the positioning of seismometers in LHN and the subarrays.

Table 1. Source data.

Shot name	Date	Time (GMT)	Shotpoint coordinates lat.	long.	Water depth (m)	Charge mass kg TNT
1A	17.6	02 00 00.09	60°07′36″	26°19′48″	75	4000
3A	17.6	04 45 00.80	63 20 32	9 14 06	140	3160
5A	17.6	03 00 00.04	56 37 08	16 51 29	55	1027
3B	19.6	02 30 01.43	63 20 32	9 14 06	140	2280
5B	19.6	03 00 00.16	56 37 09	16 51 32	55	2031
2A	24.6	02 30 00.24	61 53 30	20 44 00	72	1000
4A	24.6	03 00 00.22	58 42 45	10 49 52	70	2048
2B	26.6	02 30 00.38	62 00 02	20 29 52	118	1000
4B	26.6	03 00 00.34	54 42 44	10 49 58	70	1027

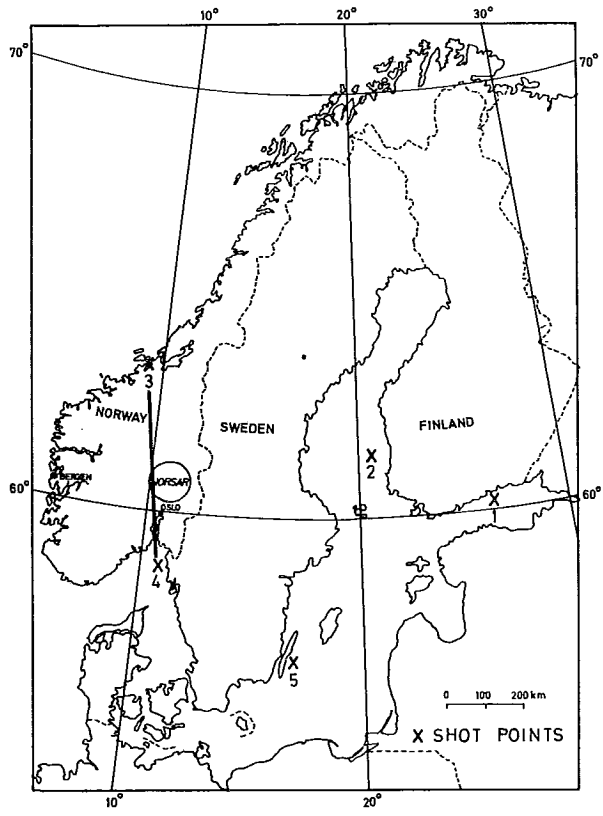

Figure 1. The distribution of shot points used in the 1969 seismic experiment.

Table 2 lists the number of records obtained at LHN and the NORSAR sub-arrays from each shot. The total number of records amounts to 215. Before the data were analysed, the records were played through an analog low-pass filter (0–12 Hz) and then converted to digital form on punched cards with a sampling rate of 50 Hz.

3. *The seismic scaling law*

The data available from the 1969 seismic experiment do not permit a detailed investigation of the seismic scaling laws for underwater explosions. However, it is

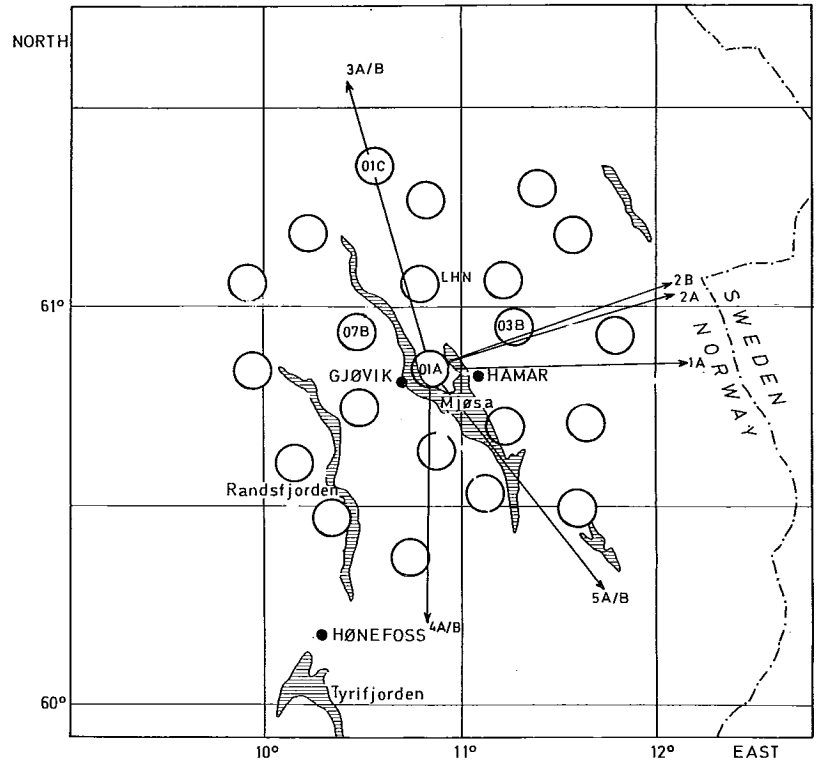

Figure 2. Location of LHN and the subarrays used. The arrows indicate the directions to the shot points.

Table 2. Number of records obtained at LHN and the NORSAR subarrays from each shot.

	1A	2A	2B	3A	3B	4A	4B	5A	5B
01A	6	6	6	6	6	6	6	6	6
03B	5	5	5	–	5	3	2	5	5
07B	5	5	5	5	5	5	5	5	5
01C	–	11	11	–	11	–	11	–	11
LHN	–	–	–	7	6	6	7	–	–
SUM	16	27	27	18	33	20	31	16	27

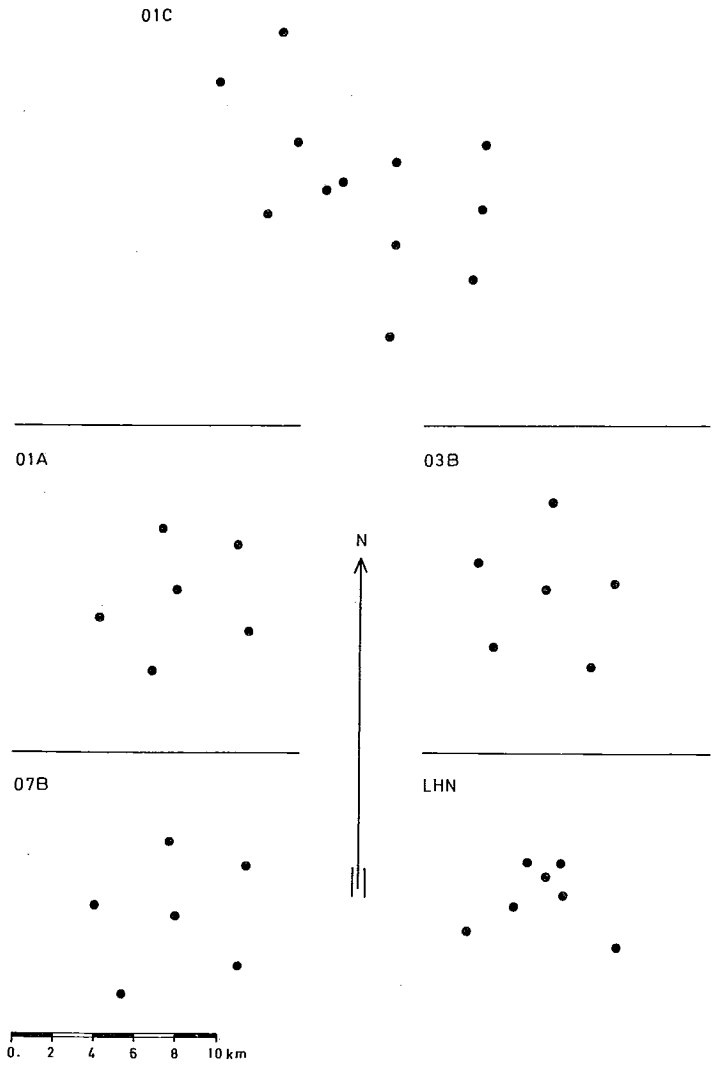

Figure 3. The distribution of seismometers in LHN and in the four subarrays used.

of interest to examine how closely the data fit a seismic scaling law approximated by a power law of the form:

$$A = C \cdot W^n \tag{1}$$

where A is the amplitude of the ground motion, C is a constant and W is the weight of the charge. The exponent n can be determined by using the observed amplitudes of the ground motion from different charges fired at the same shot point, and is given by:

$$n = \frac{\log(A_1/A_2)}{\log(W_1/W_2)} \tag{2}$$

where A_1 and A_2 are the observed ground motion amplitudes from charges of weight W_1 and W_2 respectively.

The mean value obtained for the exponent and its standard deviation is $n = 0.65 \pm 0.02$. This value is in good agreement with values previously published for underwater charges where TNT was the explosive used (MÜLLER *et al.* [7]; O'BRIEN [9]).

4. *Effect of water depth*

KANESTRØM [5] found that the pseudo-frequency (the inverse of the time difference between the first two maxima) of the P_n waves recorded at subarray 01C was mainly controlled by the water depth at the shot point. To complement this observation, the amplitude spectra were calculated for the first second of 215 seismograms (see Table 2). For all shots given in Table 1, the initial second of the seismograms include the P_n arrival, since the P_n wave was the first arrival at all seismometers. The spectra were corrected for the seismograph response and each spectrum was normalized to unity at the maximum value of the spectrum, and the normalized spectra were averaged for each shot. In this way, nine average spectra each based on 16 to 33 individual spectra were obtained (see Table 2).

Figure 4 shows average spectra for the shots 1A and 2B, and examples of average spectra obtained at the different subarrays for shot 2B are shown in Figure 5. As can be seen from Figure 4, the amplitude spectrum for shot 1A peaks at a higher frequency than that of shot 2B. This observation is unexpected in that the size of the charge in the case of shot 1A was four times as large as that for shot 2B (Table 1). Furthermore, the wave path from the shot 1A is more than 300 km longer than that for shot 2B (Table 3). It is known from experiments that larger charges displace the spectral peak towards lower frequencies (BURKHART

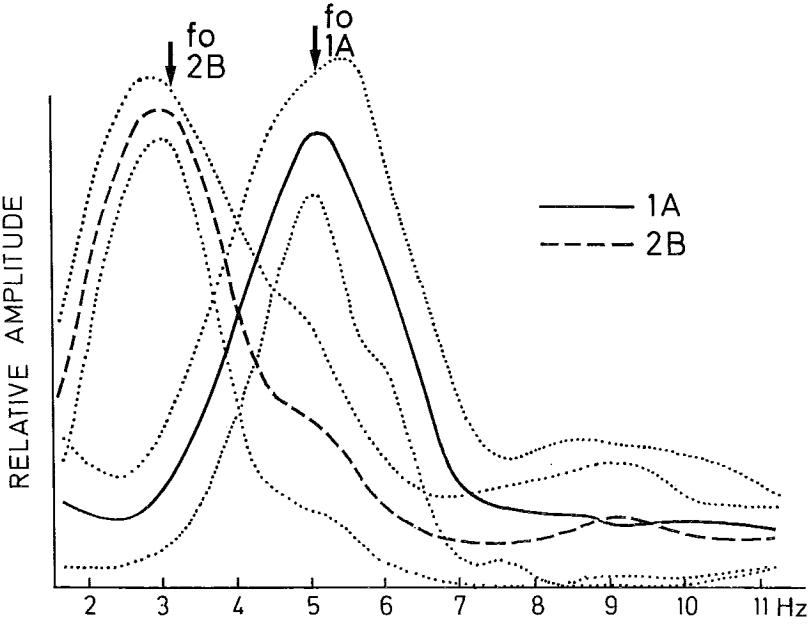

Figure 4. Average spectra for the shots 1A and 2B. The dotted lines indicate the ranges of standard deviation.

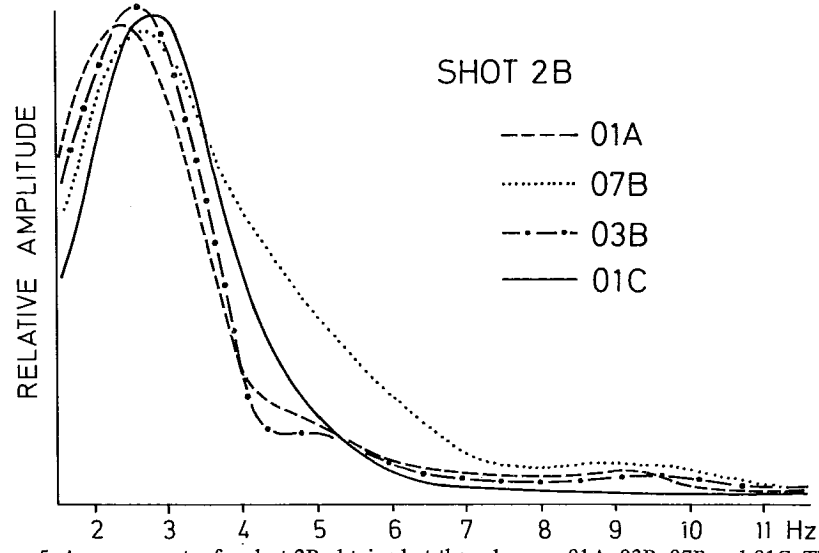

Figure 5. Average spectra for shot 2B obtained at the subarrays 01A, 03B, 07B and 01C. The spectra have not been corrected for instrumental response.

Table 3. Distances (in km) from the central seismometer in the subarrays to the shot points.

	01A	03B	07B	01C	LHN
1A	853	830	873	867	850
2A	542	516	556	541	533
2B	532	506	545	530	522
3A	293	291	276	234	270
3B	293	291	276	234	270
4A	235	246	248	293	260
4B	235	246	248	293	260
5A	584	577	603	637	602
5B	584	577	603	637	602

[3]; O'BRIEN [10]). The anelastic properties of the earth damp higher frequencies more seriously than the lower, and thus the spectral peak is enriched in lower frequencies as the wave path increases.

The difference between the spectra presented in Figure 4 is most probably due to the location of the shots. The shots 1A and 2B were fired at different water depths (Table 1). We suggest that the positions of the spectral peaks in Figure 4 are mainly the result of water reverberation. A theoretical fundamental resonance frequency (f_0) was calculated from the simple relationship:

$$f_0 = v/4h \tag{3}$$

where v is the velocity of sound in sea water (v = 1480 m/s) and h is the depth of water. In Figure 4, the theoretical frequency f_0 is indicated by an arrow. Average spectra and the theoretical fundamental resonance frequencies for shots at the four other shot points are presented in Figure 6.

A comparison of Figures 4 and 6 indicates a significant difference between the spectra of the P_n arrivals for shots 2A and 2B, even though a one-ton charge was used in both cases and the difference in the distance travelled by the waves was only about 10 km (Table 3). However, there was a difference of 46 m in the water depth at the two shot points. From the complete set of observations shown in Figure 7, there should be little doubt about the importance of water depth on the frequency of the P_n waves. The P_n arrivals from shots 2A and 2B, recorded at subarray 03B, are shown in Figure 8. For convenience, the records in Figure 8 are normalized with respect to amplitude.

The difference between the frequency at which the spectrum peaks and the theoretical fundamental resonance frequency (f_0) for shots 4A, 4B and 5B may be the result of soft sediments on the sea floor with an acoustic impedance close

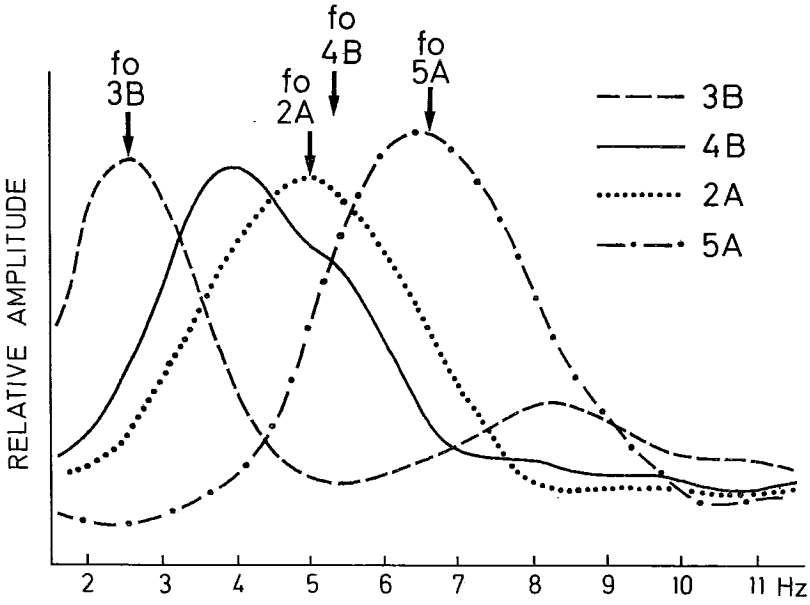

Figure 6. Average spectra for the shots 2A, 3B, 4B and 5A.

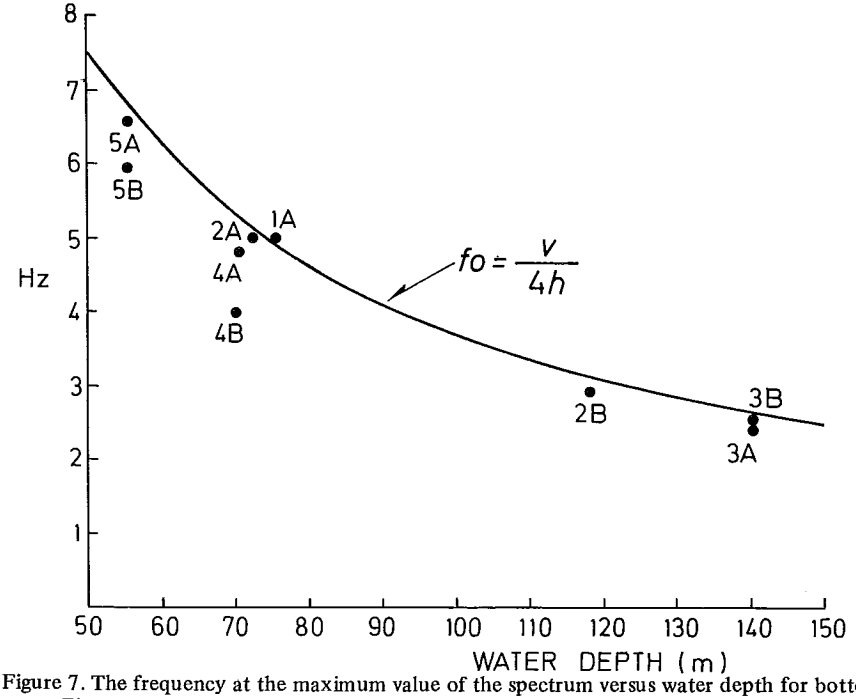

Figure 7. The frequency at the maximum value of the spectrum versus water depth for bottom-shots. The curve represents the theoretical fundamental resonance frequency $f_0 = v/4h$.

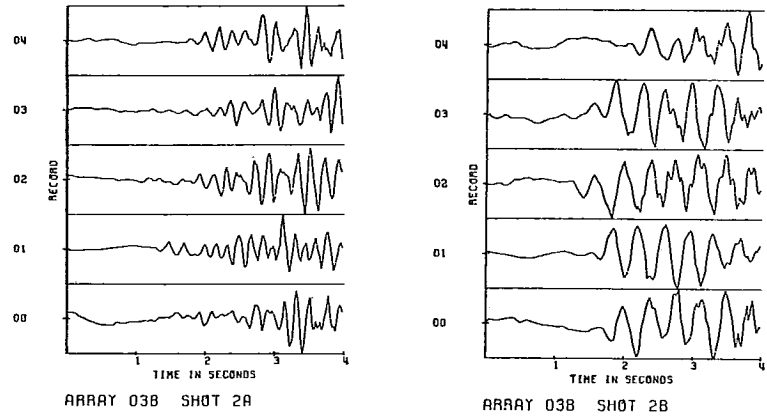

Figure 8. P_n arrivals from the shots 2A and 2B recorded at subarray 03B.

to that of sea water; reflection occurred at a level below the sea bottom. If this explanation is correct, the reflector associated with the water reverberation at shot 4B is located about 20 m below the sea floor.

Variations in amplitude spectra are frequently interpreted in terms of absorption or lateral changes in the transmission properties of a refractor, for example the Moho. The observations presented above show that variations in amplitude spectra need to be interpreted with care. With a reflection coefficient at the water-air interface of about −0.8, the original pressure pulse is followed after 0.07 to 0.19 s by a comparable negative pulse. This can explain the variation in the amplitude ratio of the second and first half-cycle shown in Figure 9. The absolute amplitudes in Figure 9 have no significance.

5. *The bubble pulse*

Secondary pressure pulses originating at the shot point after the first shock-wave emitted, result in two or more complete records superimposed on each other. It is well known that extrema in the spectra of seismic waves can result from the interference of pulses arriving in the analysed window (see NAKAMURA and HOWELL [8]; PHINNEY [11]; SISKIND and HOWELL [12]; KANESTRØM and NEDLAND [6]). Secondary pressure pulses occur in connection with underwater explosions below a certain depth, due to oscillations of the gas bubble formed. In the interpretation of seismic data from underwater shots, it is important that the bubble pulses can be recognized in the seismogram. Interference between bubble arrivals and other arrivals makes it very difficult to determine the period of the bubble pulsation

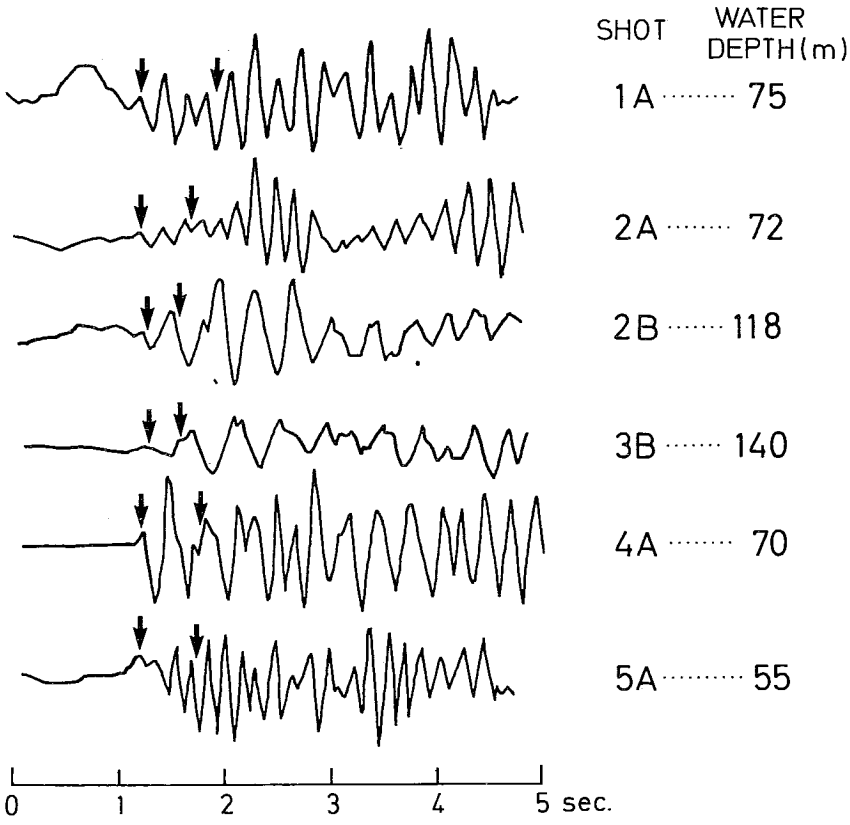

Figure 9. Examples of recordings of the different shots at subarray 07B. The first arrow indicates the arrival time of the surface reflected wave at the shot point. The second arrow indicates the onset of the first bubble pulse.

from the records. However, the approximate bubble-pulse period may be predicted using the bubble formula of Willis (COLE [4]):

$$T = C \frac{W^{1/3}}{(H + 10)^{5/6}} \tag{4}$$

where

C = 2.13 s m$^{5/6}$/kg$^{1/3}$ (for TNT)

W = charge size in kg

H = shot depth in m.

The 10 added to H is to account for atmospheric pressure. The formula given above is not valid if the shot is located close to boundary surfaces. However, equa-

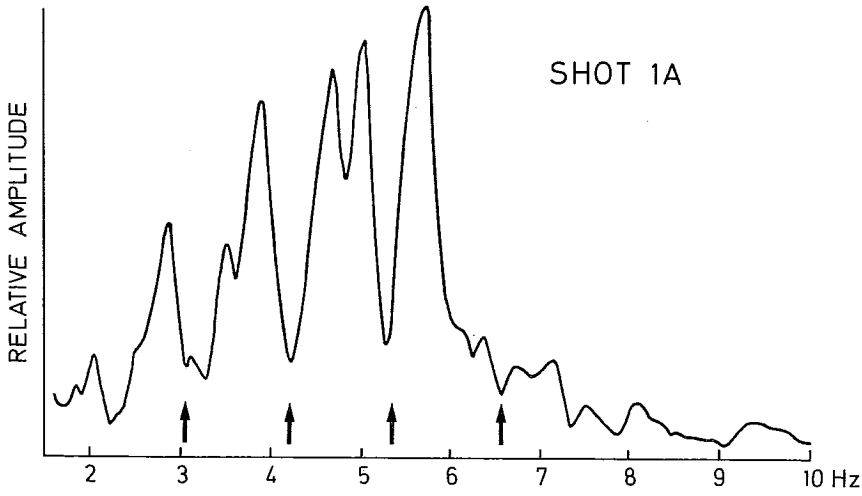

Figure 10. Average spectrum obtained for shot 1A at subarray 07B. Time interval of analysis was 6.0 s.

tions are available to correct for the effects of the free surface and bottom on the bubble-pulse period providing information is available on the characteristics of the explosives used.

Amplitude spectra were calculated for the first six seconds of 45 seismograms recorded at subarray 07B. Each spectrum was normalized to unity at the maximum value of the spectrum, and the normalized spectra were averaged for each shot. The average spectra exhibit evently spaced minima and maxima from which the bubble-pulse period can be determined. In the average spectrum obtained for shot 1A (Fig. 10), the minima and maxima occur at multiples of 1.17 Hz, corresponding to two pulses 0.85 s apart. We interpret the minima as the result of interference between arrivals from the initial shot pulse and arrivals from the bubble pulse; accordingly the bubble-pulse period for shot 1A was 0.85 s.

KANESTRØM and NEDLAND [6] found, in a similar analysis, that the frequencies at which the minima in the spectra occurred were independent of the shot-station distance. This can be demonstrated using the records obtained at the field stations along profile 3–4 (Fig. 1). Figure 11 shows the average spectrum of shot 4B recorded at subarray 07B together with the average spectrum obtained using five field stations for the same shot. The shot-station distances for the five field stations were 102, 184, 232, 320 and 414 km, and the shot-station distance for the different seismometers in subarray 07B varied between 243 and 250 km. As is seen from Figure 11, the minima occurring in the two spectra coincide, giving support to the inter-

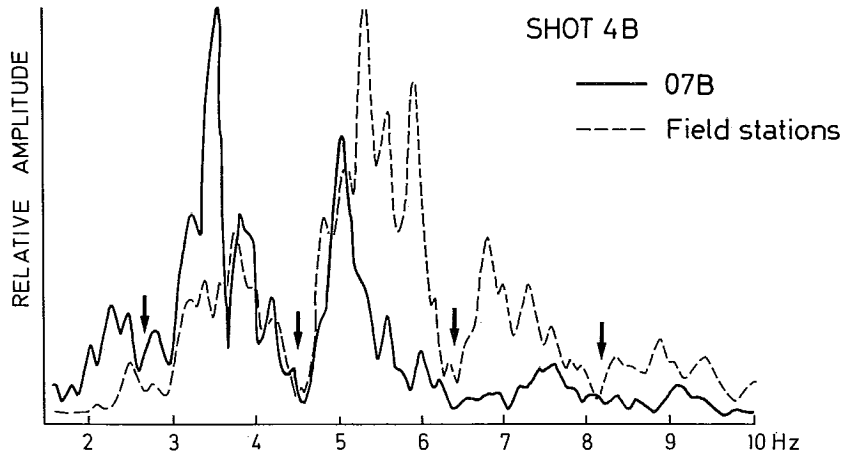

Figure 11. Average spectra for shot 4B obtained at subarray 07B (solid line), and at five field stations along profile 3–4 (dashed line).

pretation that they are the result of interference between arrivals from the initial shot pulse and arrivals from the bubble pulse. The spectra in Figures 10 and 11 have not been corrected for instrumental response, and the difference in the spectral amplitudes in Figure 11 therefore simply reflects the difference in response between the field stations and NORSAR.

The bubble-pulse period for each shot determined from the spectra are plotted in Figure 12, together with the theoretical curves computed from formula (4) for different sizes of charges. There is an excellent agreement between the experimental values and the theoretical predictions, despite the fact that no corrections have been made to the calculated values for the influence of the sea bottom. It can be seen from Figure 12 that the observed bubble-pulse periods for shots deeper than 100 m, are greater than that predicted. As already mentioned, we have not taken into account the influence of the sea floor: The net effect of this boundary is to increase the period. However, this does not only apply to the deeper shots; the necessary correction to the bubble-pulse period due to the influence of the sea bottom should increase with decreasing water depth. Nevertheless, the one-ton and two-ton shots of Figure 12 give no support to this argument.

Another phenomenon which cannot be ignored is the upward migration of the explosion bubble. The rise of the gas-bubble results in an increase in the travel time of the bubble pulse compared with the travel time for the initial shot pulse. The observed bubble-pulse period is therefore increased at a distant station. However, applying the approximate formula derived by KENNARD (cited in WILLIS [14]),

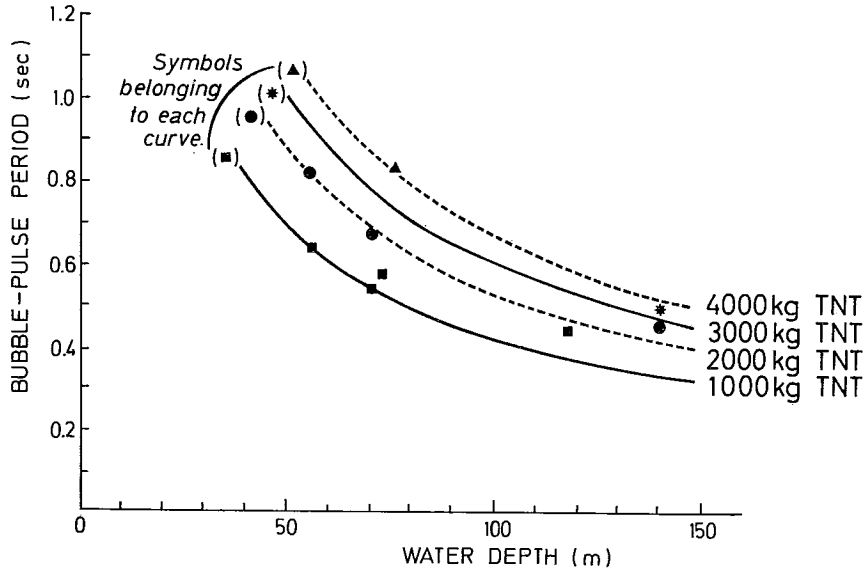

Figure 12. Measured bubble-pulse period from the six-second spectra compared with the values predicted by formula (4).

to determine the vertical migration between the initial pulse and the first bubble pulse, we find that upward movement of the gas bubble contributes less than 0.01 s to the observed bubble-pulse period for the shots analysed here.

From the discussion above, and the experimental data available in this study, it is not possible to present any final conclusion regarding the influence of the sea floor on the bubble-pulse period. It is possible that the boundary effect is negligible. In agreement with our observations, MÜLLER *et al.* [7] and BURKHARDT [3] also found that the bubble-pulse period from bottom shots agrees with that predicted by the Willis' bubble formula (4).

6. *Conclusion*

For large underwater shots, water depth affects the source spectrum in two important ways: Firstly, and most obviously, reverberations in the water layer dominates the signal spectrum; secondly water depth controls the motion of the bubble of hot gases produced by the explosion.

The amplitude spectra of the P_n arrivals from the underwater explosions in the 1969 seismic experiment are related to the water depth at the shot points. The

frequency at the maximum value of the spectrum for each shot was close to the theoretical fundamental resonance frequency $f_0 = v/4h$.

The bubble-pulse period can be determined from the evenly spaced minima and maxima in the signal spectrum using a six second window. The bubble-pulse periods obtained in this way are in agreement with those predicted by the Willis' bubble formula.

From the results obtained in the present study, it is possible to predict, or at least estimate, the spectral properties of proposed shot locations when planning seismic refraction measurements of crustal and upper-mantle structures.

REFERENCES

1. BÅTH, M., 1971: Average crustal structure of Sweden. *Pure and Appl. Geophys.* 88, 75–91.
2. BROWN, R.J., BORG, H. and M. BÅTH, 1971: Strike and dip of crustal boundaries – A method and its application. *Ibid.*, 88, 60–74.
3. BURKHARDT, H., 1964: Some physical aspects of seismic scaling laws for underwater explosions., *Geophysical Prospecting,* **12**, 192–214.
4. COLE, R.H., 1948: *Underwater explosions.* Princeton University Press.
5. KANESTRØM, R., 1973: A crust-mantle model for the NORSAR area. *Pure and Appl. Geophys.* **105**, 729–740.
6. –»– and S. NEDLAND, 1975: *Crustal structure of southern Norway.* A re-interpretation of the 1965 seismic experiment. Seismological Observatory, Univ. of Bergen.
7. MÜLLER, St., STEIN, A. and R. VEES, 1962: Seismic scaling laws for explosions on a lake bottom. *Zeitschrift f. Geophysik,* **28**, 258–280.
8. NAKAMURA, Y. and B.F. HOWELL, Jr., 1964: Maine seismic experiment: Frequency spectra of refraction arrivals and the nature of Mohorovicic discontinuity. *Bull. Seism. Soc. Am.* 54, 9–18.
9. O'BRIEN, P.N.S., 1960: Seismic energy from explosions. *Geophys. Journ.* **3**, 29–44.
10. –»– , 1969: Some experiments concerning the primary seismic pulse. *Geophysical Prospecting,* 17, 511–547.
11. PHINNEY, R.A., 1964: Structure of the earth's crust from spectral behaviour of long-period body waves. *J. Geophys. Res.* 69, 2997–3017.
12. SISKIND, D.E. and B.F. HOWELL, Jr., 1967: Scale-model study of refraction arrivals in a three-layered structure. *Bull. Seism. Soc. Am.* 57, 437–442.
13. VOGEL, A. (editor), 1971: *Deep seismic sounding in Northern Europe.* Swedish Natural Science Research Council (NFR), Stockholm.
14. WILLIS, D.E., 1963: Seismic measurements of large underwater shots. *Bull. Seism. Soc. Am.* 53, 789–809.